Monthly Notices
of the
ROYAL ASTRONOMICAL SOCIETY

MNRAS **452,** 1702–1706 (2015) doi:10.1093/mnras/stv1376

ExoMol molecular line lists – XI. The spectrum of nitric acid

A. I. Pavlyuchko,[1,2] S. N. Yurchenko[1] and Jonathan Tennyson[1]★

[1]*Department of Physics and Astronomy, University College London, London WC1E 6BT, UK*
[2]*Department of Physics, Moscow State University of Civil Engineering (MGSU), 26 Yaroslavskoye Shosse, Moscow 129337, Russia*

Accepted 2015 June 18. Received 2015 June 10; in original form 2015 April 14

ABSTRACT

Nitric acid is a possible biomarker in the atmospheres of exoplanets. An accurate line list of rotational and rotational–vibrational transitions is computed for nitric acid (HNO_3). This line list covers wavelengths longer than 1.42 μm (0–7000 cm^{-1}) and temperatures up to 500 K. The line list is computed using a hybrid variational – perturbation theory and empirically tuned potential energy and dipole surfaces. It comprises almost seven billion transitions involving rotations up to $J = 100$. Comparisons with spectra from the HITRAN and Pacific Northwest National Laboratory data bases demonstrate the accuracy of our calculations. Synthetic spectra of water–nitric acid mixtures suggest that nitric acid has features at 7.5 and 11.25 μm that are capable of providing a clear signature for HNO_3; the feature at 11.25 μm is particularly promising. Partition functions plus full line lists of transitions are made available in an electronic form as supplementary data to the article and at www.exomol.com.

Key words: molecular data – opacity – astronomical data bases: miscellaneous – planets and satellites: atmospheres.

1 INTRODUCTION

The infrared spectrum of the nitric acid molecule, HNO_3, is of astrophysical interest because of the growing interest in the study of atmospheres of extrasolar planets. In particular, this interest is particularly linked to that of the planets with Earth-like atmospheres with a high content of nitrogen and oxygen. Nitric acid can be clearly observed in the earth's atmosphere from space (Cooper et al. 2011) as it has a number of features which lie in water transparency windows. Its spectrum constitutes a possible biomarker as its existence is indicative of the presence of free oxygen and nitrogen, both of which lack strong spectral signatures at long wavelengths. It is also thought likely to pay an important role in nitrogen fixation on Mars and other Earth-like planets (Summers & Khare 2007). It has also been suggested that γ-ray bursts could produce large quantities of HNO_3 in the atmospheres of Earth-like planets (Thomas & Melott 2006). Nitric acid is a constituent of atmospheric ices on Earth and is thought likely to be present in the ice crust of Europa (Cooper et al. 2011). Its formation in interstellar ammonia ices has also been suggested (Zanchet et al. 2013), although nitric acid has yet to be observed in the interstellar medium.

Given the importance of HNO_3 in the Earth's atmosphere, its infrared spectrum has been well studied in the laboratory. However, many of these spectra remain incompletely analysed with very few assignments to transitions at wavelengths shorter than 5 μm. This lack of assignment means that the spectra cannot be used for spectral simulations at temperatures other than the one of the original experiment. Spectral data on HNO_3 is only given in the HITRAN data base (Rothman et al. 2013) for up to 1770 cm^{-1} (wavelengths longer than 5.6 μm). At shorter wavelength the Pacific Northwest National Laboratory (PNNL) data base (Sharpe et al. 2004) provides infrared cross-sections, but again these are only valid at the temperature for which they are recorded. Our results compare favourably with these sources, although this comparison shows both have their limitations (Pavlyuchko, Yurchenko & Tennyson 2015a).

The ExoMol project aims at generating comprehensive line observation and modelling atmospheres of exoplanets and other hot astronomical objects such as brown dwarfs and cool stars; its aims, scope and methodology have been summarized by Tennyson & Yurchenko (2012). The project has provided rotation–vibration line lists for a number of polyatomic molecules such as HCN (Barber et al. 2014), H_2S (Azzam, Yurchenko & Tennyson, in preparation), PH_3 (Sousa-Silva et al. 2015), H_2CO (Al-Refaie et al. 2015) and CH_4 (Yurchenko & Tennyson 2014; Yurchenko et al. 2014). None of these molecules contains more than two heavy atoms and the only pentatomic molecule considered, methane, has four hydrogens and high symmetry. It is clear that computing a comprehensive, temperature-dependent line list for HNO_3 represents a considerable computational challenge. To address this challenge we have developed a hybrid variational–perturbation theory procedure for computing spectra of such molecules (Pavlyuchko, Yurchenko & Tennyson 2015b) and have tested this for room-temperature nitric acid spectra (Pavlyuchko et al. 2015a). In this work we present a comprehensive line list for nitric acid which should be valid for temperatures up to 500 K. Given that nitric acid is only likely to

★E-mail: j.tennyson@ucl.ac.uk

exist in atmospheres which also contain water, we explicitly consider regions where HNO_3 spectra are likely to be observable in a humid atmosphere.

2 METHOD

Rotation–vibration line lists were generated using the program ANGMOL (Gribov & Pavlyuchko 1998; Pavlyuchko et al. 2015b). Although ANGMOL is designed to solve the nuclear motion problem for polyatomic molecules using a hybrid variational–perturbation theory method, it actually provides a complete environment for performing the line list calculations. ANGMOL automatically generates the inputs required to drive the appropriate ab initio electronic structure program, here the quantum chemistry package MOLPRO (Werner et al. 2012), to provide the necessary inputs for the nuclear motion calculations (potential energy, Hessian matrix and dipole moments). It also automatically adjusts both the potential energy surface (PES) and dipole moment function (DMF), which are represented as Taylor-expansions about equilibrium, to reproduce observed line positions and intensities using the method of regularization (Tikhonov & Arsenin 1979; Gribov & Dementiev 1992). This method uses constraints provided by the initial ab initio calculations to allow many more parameters to be varied than there are experimental data. For full details of the fits and associated surfaces, see Pavlyuchko et al. (2015a).

ANGMOL solves a Watson-like nuclear motion Hamiltonian expressed in internal curvilinear vibrational coordinates in three steps. First the rotation-less ($J = 0$) vibrational problem is solved in a basis of Morse oscillators for the stretches and harmonic oscillators for the bends by direct diagonalization of a Hamiltonian matrix for low-lying vibrational states with contributions from higher states (basis functions) included using perturbation theory. In the second step, rotational problems for each vibrational state are solved using the eigenvectors from the vibrational problem and Wigner rotation matrices. An Eckart embedding is used to minimize Coriolis interactions which are again introduced using perturbation theory. The final step computes transition intensities; this step reduces the size of the calculation by predicting which transitions will be too weak to make a significant contribution and not calculating them. Transitions whose intensity is less than 10^{-12} km mole^{-1} ($\approx 10^{-31}$ cm molecule^{-1}) were neglected. Integrals over the kinetic energy operator, PES and DMF are all simplified by the use of Taylor expansions for the operators. Here the PES and DMF were represented as fourth-order and second-order expansions, respectively. Further details of the calculation can be found in Pavlyuchko et al. (2015a).

Our aim was to compute an HNO_3 line list which is complete up to 7000 cm^{-1} (longwards of 1.42 μm) for temperatures up to 500 K. For this we considered energy levels up to 9000 cm^{-1} and rotational states with J up to 100. $J = 100$ corresponds to a rotational excitation of about 2130 cm^{-1}.

The initial vibrational ($J = 0$) problem was solved using vibrational basis sets with polyad number 14. By this we mean that all combinations of functions were included when the sum of the orders of the polynomials was less than or equal to 14. The size of the basis required increases combinatorially with polyad number N: for HNO_3, which has nine vibrational modes, the size of the basis is given by the binomial coefficient ${}_{N+9}C_9$ which equals 817 190 for $N = 14$ and 48 620 for $N = 9$. Matrices constructed with polyad 9 were explicitly diagonalized once the effects of higher states were included using perturbation theory, see Pavlyuchko et al. (2015a) for further details. These calculations gave a total of 22 049 vibrational states below 9000 cm^{-1}.

Table 1. Partition function, $Q(T)$, of as a function of temperature.

T (K)	$Q(T)$ This work	$Q(T)$ Fischer et al. (2003)
60	15 032.00	15 010
110	37 418.02	37 374
160	67 172.12	67 105
210	107 006.55	106 880
260	161 987.99	161 650
310	239 197.27	238 250
360	348 081.08	345 830
410	500 933.14	496 570
460	713 230.66	706 730

Rotationally excited states were computed based on calculation which only considered up to polyad 7 but with the vibrational band origins fixed by the larger $J = 0$ calculation. This gave 9477 states lying below 7000 cm^{-1} of which intensity considerations (see Pavlyuchko et al. 2015a for details) showed that only 1715 need to be considered explicitly. No transition whose intensity was less than 10^{-31} cm molecule^{-1} was considered.

Our final line list links 17 494 715 vibration-rotation energy levels with 6 722 136 109 transitions.

Temperature-dependent partition functions for HNO_3 were calculated by explicitly summing all the calculated energy levels. Table 1 compares our results with those used by HITRAN (Fischer et al. 2003). The agreement is very good; our results are systematically slightly larger by less than 0.2 per cent at low temperatures rising to 0.9 per cent at 500 K. This increase is probably due to our better treatment of anharmonic effects, particularly in the large-amplitude, low-frequency OH torsional mode. A file containing the partition function with 1 K step for temperatures up to 500 K is given in supplementary material.

3 RESULTS

The line list contain almost seven billion transitions. For compactness and ease of use, it is divided into separate energy level and transitions files. This is done using standard ExoMol format (Tennyson, Hill & Yurchenko 2013) which is based on a method originally developed for the BT2 line list (Barber et al. 2006). Extracts from the start of the files are given in Tables 2 and 3. The full line list can be downloaded from the CDS, via ftp://cdsarc.u-strasbg.fr/pub/cats/J/MNRAS/, or http://cdsarc.u-strasbg.fr/viz-bin/qcat?J/MNRAS/. The line lists and partition function, as well as the absorption spectrum given in cross-section format (Hill, Yurchenko & Tennyson 2013), can all be obtained from there as well as at www.exomol.com.

Fig. 1 compares our calculations with the cross-sections given in the PNNL data base (Sharpe et al. 2004). More detailed comparisons with both PNNL and HITRAN (Rothman et al. 2013) are given by Pavlyuchko et al. (2015a).

Given that HNO_3 is being considered as possible biomarker and that any biomarker will probably have to be observed in a humid atmosphere, we consider a number of mixed water – nitric acid spectra. Fig. 2 gives an overview of such spectra which have been constructed using water from HITRAN with 2 per cent HNO_3 added for 300 and 500 K. As is well known, water absorptions dominate much of the infrared. However, HNO_3 features are clearly visible at about 7.5 and 11.2 μm. These are precisely where HNO_3 is clearly

Table 2. Extract from the state file for HNO_3. Full tables are available from http://cdsarc.u-strasbg.fr/cgi-bin/VizieR?-source=J/MNRAS/. Here n: state counting number; $\tilde{E}$: state energy in cm^{-1}; g: state degeneracy; J: rotational quantum number; Γ: total symmetry; v_1, v_2, v_3, v_4, v_5, v_6, v_7, v_8, v_9: vibrational quantum numbers.

n	$\tilde{E}$	g	J	Γ	v_1	v_2	v_3	v_4	v_5	v_6	v_7	v_8	v_9
1	0.000 000	6	0	A'	0	0	0	0	0	0	0	0	0
2	458.200 000	6	0	A''	0	0	0	0	0	0	0	0	1
3	580.300 000	6	0	A'	0	0	0	0	0	0	0	1	0
4	646.450 000	6	0	A'	0	0	0	0	0	0	1	0	0
5	763.100 000	6	0	A''	0	0	0	0	0	1	0	0	0
6	879.050 000	6	0	A'	0	0	0	0	1	0	0	0	0
7	896.300 000	6	0	A'	0	0	0	0	0	0	0	0	2
8	1038.000 000	6	0	A''	0	0	0	0	0	0	0	1	1
9	1100.800 000	6	0	A''	0	0	0	0	0	0	1	0	1
10	1148.975 745	6	0	A'	0	0	0	0	0	0	0	2	0
11	1205.600 000	6	0	A'	0	0	0	0	0	1	0	0	1
12	1213.857 206	6	0	A'	0	0	0	0	0	0	1	1	0
13	1275.720 926	6	0	A'	0	0	0	0	1	0	1	0	0
14	1289.000 000	6	0	A''	0	0	0	0	0	0	0	0	3
15	1303.100 000	6	0	A'	0	0	0	1	0	0	0	0	0
16	1325.650 000	6	0	A'	0	0	1	0	0	0	0	0	0
17	1340.608 559	6	0	A''	0	0	0	0	0	1	0	1	0
18	1343.600 000	6	0	A''	0	0	0	0	1	0	0	0	1
19	1403.878 302	6	0	A''	0	0	0	0	0	1	1	0	0
20	1450.282 008	6	0	A'	0	0	0	0	1	0	0	1	0

Table 3. Extracts from the transitions file for HNO_3. Full tables are available from http://cdsarc.u-strasbg.fr/cgi-bin/VizieR?-source=J/MNRAS/. Here F: upper state counting number; I: lower state counting number; A_{FI}: Einstein-A coefficient in s^{-1}.

F	I	A_{FI}
14 516 084	14 516 083	4.5130E−10
14 516 265	14 516 264	8.1767E−10
14 515 899	14 515 898	1.8398E−09
14 516 082	14 516 081	2.4872E−08
14 516 263	14 516 262	2.8596E−08
14 515 897	14 515 896	7.7843E−08
14 516 080	14 516 079	6.5506E−07
14 516 261	14 516 260	6.2021E−07
14 515 895	14 515 894	1.5810E−06
14 516 078	14 516 077	7.7309E−06
14 516 080	14 516 078	7.1042E−06
14 515 895	14 515 893	1.5567E−05
14 516 259	14 516 258	5.9759E−06
14 515 897	14 515 895	1.8498E−05
14 515 893	14 515 892	1.4427E−05
14 516 261	14 516 259	1.2759E−05

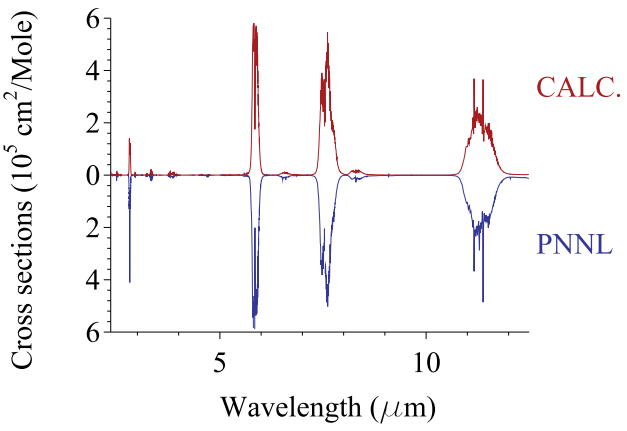

Figure 1. Comparison of our computed spectrum (Calc) with cross-sections from the PNNL data base (Sharpe et al. 2004) at a temperature of 298 K. Cross-sections were generated from our line list using a Voigt profile with a Doppler and pressure-broadening widths both set to 0.075 cm^{-1}.

seen in our own atmosphere from space (Blecka & De Maziere 1996).

Figs 3 and 4 give detailed comparisons for the two regions in question. The spectrum in the 7.5 μm region shows a clear, regular spectral signature of HNO_3 but would require both a significant fraction of HNO_3 present and high resolution for a successful detection. When viewed in the Earth's atmosphere this region also shows strong absorption lines due to CO_2, although there are not enough of these to mask the HNO_3. The 11.2 μm region is actually much more promising. The figure is drawn for only a trace concentration of HNO_3 (0.01 per cent of water), much less than is present in the Earth's atmosphere. Furthermore there is a distinct HNO_3 band centred about 11.25 μm and a feature 11.38 μm which should be visible (possibly blended together) at lower resolution. This would appear to be the most promising region for an HNO_3 detection. We note that there is one further HNO_3 band clearly visible in Fig. 2 at about 3 μm. This feature is a blend of the $2\nu_3$ overtone (band centre at 3404.4 cm^{-1}), and the $\nu_2 + \nu_4$ (2998.5 cm^{-1}) and $\nu_2 + \nu_3$ (3022.1 cm^{-1}) combination bands. This compound band sits in a window in the water spectrum but is not particularly prominent in the spectrum of the Earth's atmosphere, presumably because it is actually significantly weaker than the features at 11.2 and 7.5 μm.

4 CONCLUSIONS

As part of the ExoMol project we have computed a comprehensive line list for the possible biomarker nitric acid applicable to temperatures up to 500 K. To do this we have had to develop a

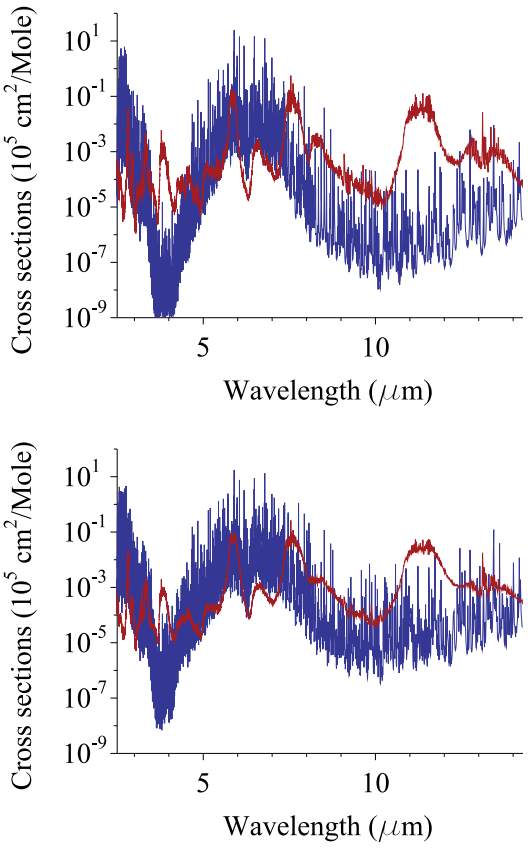

Figure 2. Temperature-dependent absorption spectra of a nitric acid (smooth curve) and water vapour (spiky curve) mixture. Spectra are for 2 per cent nitric acid at 300 K (upper) and 500 K (lower). The water spectra show a strong window around 4 μm.

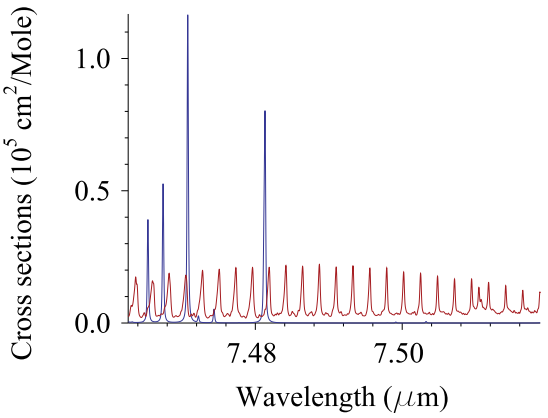

Figure 3. Absorption spectrum of a nitric acid (regular set of lines) and water vapour (four strong lines) mixture in the 1330 – 1340 cm^{-1} region. The spectrum is for 300 K with a concentration of 2 per cent nitric acid.

novel methodology capable of treating the anharmonic motions of a heavy five-atom molecule (Pavlyuchko et al. 2015a,b). The line lists, which contains almost seven billion lines, can be downloaded from the CDS, via ftp://cdsarc.u-strasbg.fr/pub/cats/J/MNRAS/, or http://cdsarc.u-strasbg.fr/viz-bin/qcat?J/MNRAS/, or from www.exomol.com.

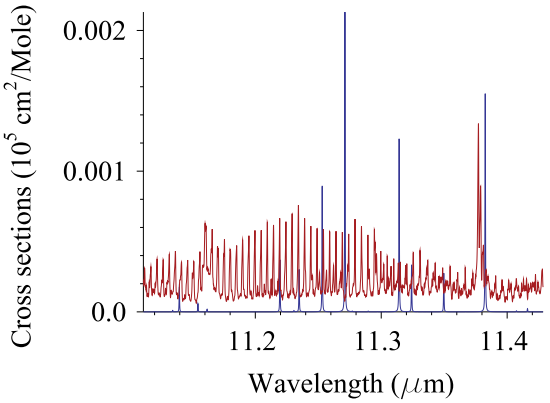

Figure 4. Absorption spectrum of a nitric acid (regular set of lines) and water vapour (isolated lines) mixture in the 875–900 cm^{-1}. The spectrum is for 300 K with a trace concentration of 0.01 per cent nitric acid.

Simulated spectra for a water-rich atmosphere suggest that there is real prospect of detecting trace quantities of nitric acid in the 11.25 μm region.

ACKNOWLEDGEMENTS

This work is supported by ERC Advanced Investigator Project 267219. The authors acknowledge the use of the UCL Legion High Performance Computing facility (Legion@UCL) and associated support services in the completion of this work.

REFERENCES

Al-Refaie A. F., Yurchenko S. N., Yachmenev A., Tennyson J., 2015, MNRAS, 448, 1704
Barber R. J., Tennyson J., Harris G. J., Tolchenov R. N., 2006, MNRAS, 368, 1087
Barber R. J., Strange J. K., Hill C., Polyansky O. L., Mellau G. C., Yurchenko S. N., Tennyson J., 2014, MNRAS, 437, 1828
Blecka M. I., De Maziere M., 1996, Ann. Geophys., 14, 1103
Cooper M. et al., 2011, J. Geophys. Res.: Atmos., 116, D12306
Fischer J., Gamache R. R., Goldman A., Rothman L. S., Perrin A., 2003, J. Quant. Spectrosc. Radiat. Transfer, 82, 401
Gribov L. A., Dementiev V. A., 1992, J. Appl. Spectrosc., 56, 709
Gribov L. A., Pavlyuchko A. I., 1998, Variational Methods for Solving Anharmonic Problems in the Theory of Vibrational Spectra of Molecules. Nauka, Moscow (in Russian)
Hill C., Yurchenko S. N., Tennyson J., 2013, Icarus, 226, 1673
Pavlyuchko A. I., Yurchenko S. N., Tennyson J., 2015a, J. Chem. Phys., 142, 094309
Pavlyuchko A. I., Yurchenko S. N., Tennyson J., 2015b, Mol. Phys. (doi: 10.1080/00268976.2014.992485)
Rothman L. S. et al., 2013, J. Quant. Spectrosc. Radiat. Transfer, 130, 4
Sharpe S. W., Johnson T. J., Sams R. L., Chu P. M., Rhoderick G. C., Johnson P. A., 2004, Appl. Spectrosc., 58, 1452
Sousa-Silva C., Al-Refaie A. F., Tennyson J., Yurchenko S. N., 2015, MNRAS, 446, 2337
Summers D. P., Khare B., 2007, Astrobiology, 7, 333
Tennyson J., Yurchenko S. N., 2012, MNRAS, 425, 21
Tennyson J., Hill C., Yurchenko S. N., 2013, in Gillaspy J. D., Wiese W. L., Podpaly Y. A., eds, AIP Conf. Proc. Vol. 1545, Eighth International Conference on Atomic and Molecular Data and their Applications: ICAMDATA-2012. Am. Inst. Phys., New York, p. 186
Thomas B. C., Melott A. L., 2006, New J. Phys, 8, 120
Tikhonov A. N., Arsenin V. Y., 1979, Bull. Am. Math. Soc., 1, 521

Werner H.-J., Knowles P. J., Knizia G., Manby F. R., Schütz M., 2012, WIREs Comput. Mol. Sci., 2, 242
Yurchenko S. N., Tennyson J., 2014, MNRAS, 440, 1649
Yurchenko S. N., Tennyson J., Bailey J., Hollis M. D. J., Tinetti G., 2014, Proc. Natl. Acad. Sci., 111, 9379
Zanchet A., Rodriguez-Lazcano Y., Galvez O., Herrero V. J., Escribano R., Mate B., 2013, ApJ, 777, 26

SUPPORTING INFORMATION

Additional Supporting Information may be found in the online version of this article:

hno3.pf
(http://mnras.oxfordjournals.org/lookup/suppl/doi:10.1093/mnras/stv1376/-/DC1).

Please note: Oxford University Press are not responsible for the content or functionality of any supporting materials supplied by the authors. Any queries (other than missing material) should be directed to the corresponding author for the article.

This paper has been typeset from a TEX/LATEX file prepared by the author.